Crack Tracking in Reinforced Masonry Walls: A Pilot Study to Find the Best Predictor of the Drift Experienced by Damaged Walls

Gonzalo Lema[i], Sebastián Calderón[ii], Antonio Suazo[iii], and Cristián Sandoval[iv]

ABSTRACT

Evidence suggests that shear walls might be more damaged than they appear after a seismic event. Many cracks become undetectable once the load is removed, representing a real challenge for post-earthquake structural assessments. Accordingly, this research proposes a methodology to assess and quantify the development of visible damage in BJR-PG-RM walls subjected to in-plane cyclic loads. The study aims to quantify cracks observed at peak deformation and the residual cracks remaining after load removal. This allows the assessment and quantification of the effective damage incurred by the wall following a simulated earthquake.

A detailed damage characterization was conducted on three test walls, extracting surface damage indicators such as crack width, crack length, internal crack area, and bounding box area of cracks. These damage parameter indices were obtained at different load stages of the in-plane cyclic load test. Observations revealed that walls can conceal up to 35% of the visible damage upon unloading. This capacity to conceal visible damage diminishes after the wall reaches its peak shear resistance. This study also highlights that relying solely on maximum crack width is ineffective in accurately characterizing the damage state of a wall. It is not capable of reliably predicting whether a wall has reached its peak shear resistance. In contrast, crack length and internal crack area emerge as suitable candidates for damage characterization, exhibiting a consistent progression that enables clear differentiation between damage states before and after reaching peak shear resistance. This study presents a novel methodology for assessing and evaluating damage in masonry walls under in-plane cyclic loading. It contributes to a deeper understanding of the damage progression in masonry shear walls, providing valuable damage characterization.

KEYWORDS

damage assessment, damage progression, in-plane cyclic loads, crack development, closing cracks

[i] PhD student, Universidad de Concepción, Concepción, Chile, glema2017@udec.cl
[ii] Assistant Professor, Universidad de Concepción, Concepción, Chile, sebastian.calderon@udec.cl
[iii] PhD student, Pontificia Universidad Católica, Santiago, Chile, asuazo1@uc.cl
[iv] Associate Professor, Pontificia Universidad Católica, Santiago, Chile, cristian.sandoval@uc.cl

INTRODUCTION

The behavior of masonry structures under cyclic loads, such as those induced by earthquakes, is a critical aspect that needs to be evaluated in existing structures. The safety of occupants usually depends on the criteria adopted by engineers in post-earthquake inspections, although it has been recognized that inaccuracy might be present. For instance, in New Zealand, a five-story reinforced concrete building structured with beam-column frames and a shear wall core sustained damage during the 2010 Canterbury earthquake (Mw=7.1). The shear walls exhibited crack widths of up to 0.5 mm and were injected with epoxy resin into cracks wider than 0.2 mm. However, two months later, another earthquake struck the region (Mw=6.3), causing the retrofitted building to collapse with devastating consequences (Elwood, 2013). This tragic event highlights the critical implications of inaccurate damage evaluation methodologies and underscores the urgent need for reliable predictors of structural damage to ensure safer buildings after earthquake events.

A crucial aspect of evaluation methodologies is to characterize the damage evolution in masonry structural elements, particularly in structural shear walls. The predominant failure mode in shear walls is characterized by a brittle diagonal cracking failure, limited energy dissipation capacity, and a quick decline in lateral stiffness [1]. In these elements, the superficial crack pattern is a visible indicator for evaluating damage. Murcia-Delso & Shing [2] defined two damage states for shear-dominated masonry walls (moderate, DS4, and severe, DS5). The moderate damage state is characterized by the formation of the first significant diagonal shear crack, and the severe damage is characterized by the existence of numerous diagonal cracks, crushing of masonry units, and even separation at the wall base. These damage states are suitable damage indicators when studying laboratory-tested walls where all response variables (e.g., forces, displacements, deformations) are being measured, although difficulties arise when this methodology is required to be used for real study cases.

In this regard, the quantification of cracks on shear wall surfaces can serve as a crucial input regarding the post-seismic damage assessment of buildings. Most existing post-earthquake assessment protocols base the damage evaluation on parameters such as maximum crack widths, crack distributions, and qualitative analysis of the analyzed structure elements [3,4]. These visual damage assessment methodologies for buildings have proven to have several shortcomings and inconveniences [5]. Moreover, some authors note that a significant number of cracks, visible only during the application of force, often visibly disappear once the load is removed [6]. This phenomenon has not been properly addressed in the literature, potentially leading to inaccurate damage assessments of shear walls during post-seismic evaluations and misestimation of the residual strength of walls. This is clearly a safety issue that requires further investigation.

Accordingly, this research aims to reduce the subjectiveness of damage assessments by quantifying surface damage observed at unloaded stages of cyclic shear loads of reinforced masonry walls and correlating it with the incurred damage level at the loaded state. Furthermore, different visible damage indexes are studied to determine the most suitable for this methodology. This proposed assessment methodology might be extended to shear walls of different materials, although it is tested with experimental data of reinforced masonry shear walls built according to Chilean construction practices.

PROPOSED METHODOLOGY FOR DAMAGE ASSESSMENT

The overview of the assessing methodology adopted is presented in Fig. 1. The first step is to recognize the cracked areas in each photograph. The issue is that masonry surfaces exhibit non-homogeneous surfaces with high noise levels, which poses challenges for automatic crack detection methods (e.g., deep learning models (e.g., [7]). Therefore, a manual outlining approach, performed using photograph edition software, was preferred since it ensures accurate and consistent outcomes. The size of the acquired images was 6000 x 4000 pixels, which resulted in a ratio of 0.87 millimeters per pixel.

Following this, image processing techniques are applied to binarize the image of cracks, facilitating the subsequent treatment analysis for the algorithm. Once the crack pattern is extracted as a binary logical matrix, an algorithm is developed to identify the evolution of cracks during the test. This provides each crack entity with properties such as location, centroid, boundaries, length, area, and a unique identification tag. It is worth noting that, to define the length and shape of each crack, crack nodes are eliminated from the map. Then, the algorithm is employed to identify and compute key parameters of the crack pattern for each load condition, such as maximum crack width, average crack width, total area covered by cracks, total crack length, and the total effective area of the bounding box enclosing the cracks, which are described below. These parameters are obtained for the pictures taken at the maximum of each load cycle (only in the push load direction of the test). The latter procedure is repeated at the unloaded condition (zero drift position) that is achieved afterward as the load protocol continues. These crack patterns are extracted to evaluate the correlation between the applied drift and the resulting damage, both during loading and its immediate unloading phases.

Subsequently, the correlation between the calculated crack parameters and the respective demand parameters (e.g., imposed load, displacement, and story-drift ratio) is assessed to get an insight into the behavior of the crack development under load and unloaded conditions.

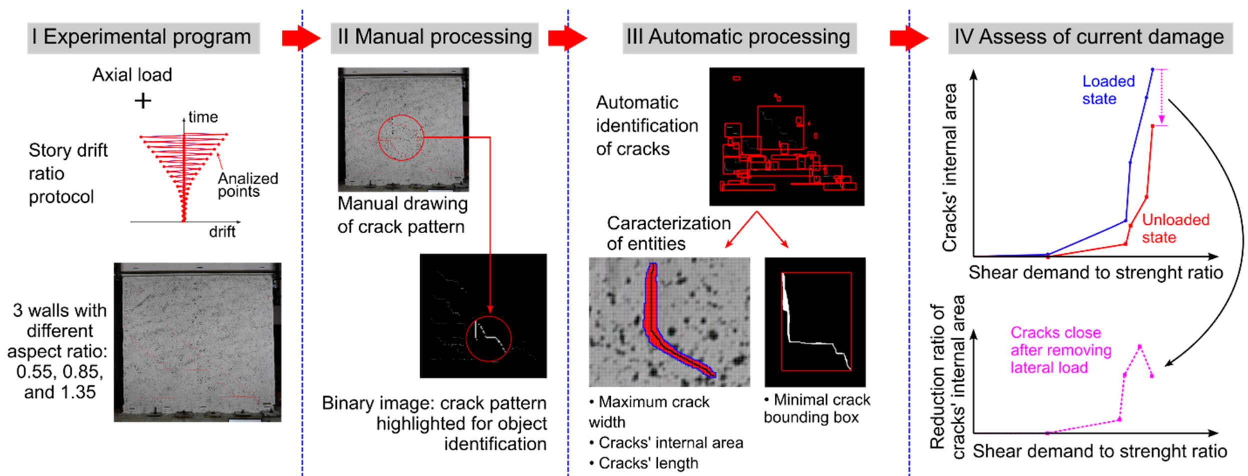

Figure 1. Adopted approach and methodology for crack development analysis in shear walls subjected to in-plane cyclic loads.

The novelty of this approach lies in assessing the true quantitative extent of damage incurred by the wall during the loading phase, inferred from the crack patterns observed after the load is removed. This is particularly important because it tries to assess if the wall may sustain more damage than visible damage when the load is removed, such as during post-seismic inspections. However, the method also has some drawbacks. For example, the resolution of photographs can directly affect the sensitivity of the method, as the low resolution will impede the identification of narrow cracks. Furthermore, human errors during the process of manually drawing the crack pattern in each photograph can significantly influence the analysis outcomes. Large working sessions can tire the operator, potentially leading to inconsistencies during the process. Additionally, performing this process with different operators can also introduce variability that will pollute the final results.

Damage index: Maximum crack width

The maximum crack width is defined as the maximum distance between the points of the crack skeleton (central points) and the outer perimeter of the crack. This distance is calculated at each point of the skeleton and considers the length (in pixels) in eight different directions: right, down-right, down, down-left, left, upper-left, up, and upper-right. These directions can be observed in Fig. 2(a), where the binary representation of a crack and the main directions from a point of the crack skeleton are shown. Subsequently, the minimal central point-to-perimeter distance is determined. The width of the crack at this skeleton point is considered twice that distance. Then, the maximum width of the crack entity is identified as the maximum of all thicknesses measured along the crack. Afterward, all maximum crack widths are compared, and the crack with the greatest thickness across the entire wall surface is selected at each measurement stage as a parameter for measuring visible surface damage.

Damage index: Total crack length

The total crack length is defined as the sum of the lengths of all individual cracks present at a given load stage. In Fig. 2(a), the length of an individual crack is measured as the length of its skeleton.

Damage index: Total internal crack area

The internal cracked area (A_{int} in mm2, Eq. [1]) is obtained for each measurement stage as the sum of pixels present in each crack (px_i) in an image with n cracks, multiplied by a conversion factor from squared pixels to millimeters ($f_{px^2 \to mm^2}$).

(1) $$A_{int}\,(mm^2) = \bigcup_{i=1}^{n} px_i \cdot f_{px^2 \to mm^2}$$

Damage index: Bounding cracked area

The bounding cracked area for each load stage is determined as the union of the areas of the n rectangular polygons that enclose each crack entity ($A_{g,i}$). The rectangular bounding polygon area for a given crack is depicted in Fig. 2(b). The polygon formed by all individual bounding rectangles (Fig. 2(c)) is the minimum rectangle that completely encloses the boundaries of each crack and also represents the section of the wall affected by the cracks. It is worth mentioning that the total bounding crack area calculation considers overlapping areas only once.

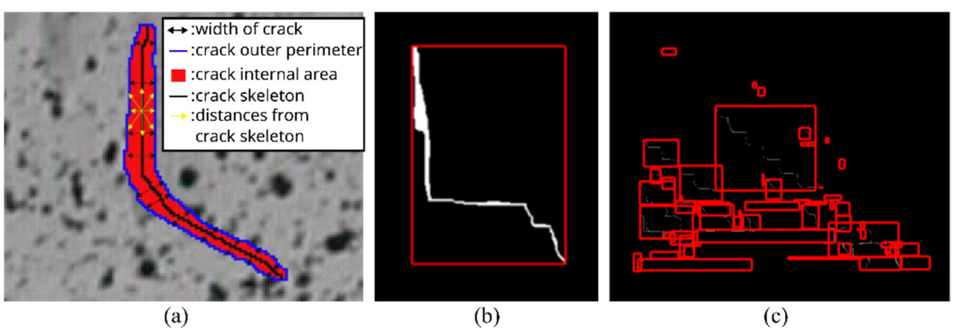

Figure 2. (a) Features of a crack, (b) Bounding cracked area for each crack, and (c) total bounding cracked area for a measurement stage.

STUDY CASES

Although the proposed assessment methodology is general, the test data corresponds to reinforced masonry shear walls following typical Chilean construction practices (also used in other Latin American countries). The test data corresponds to partially grouted reinforced masonry with horizontal reinforcement embedded in the joints (BJR-PG-RM, Bed Joint Reinforced Partially Grouted Reinforced Masonry).

The methodology is applied to three full-scale BJR-PG-RM shear walls constructed with multi-perforated clay units (14 cm thick) and tested under incremental alternated in-plane loading by Calderón et al. [8]. The walls CLBW01, CLBW02, and CLBW03 had different aspect ratios, varying from 0.55 to 1.35. These case studies were chosen because of their different aspect ratio, a variable relevant to the lateral response of walls. Specifically, the lateral resistance decreases proportionally with the aspect ratio irrespective of the horizontal reinforcement ratio and axial pre-compression load [1]. Also, the aspect ratio influenced the stress-strain patterns developed in the walls, which reflected in the crack patterns [8]. During tests, walls were monitored using different sensors, which allowed to register lateral displacements and forces, and also pictures at regular intervals of 5 seconds were taken. An alternated lateral displacement protocol was used, which allowed taking pictures at the maximum displacement of each loading cycle and also at zero displacement. The wall designs comply with the provisions of the current Chilean standard for reinforced masonry (NCh1928Of1993Mod.2009 [9]). Table 1 and Fig. 3 provide the characterization and design parameters of the three shear walls analyzed in this study.

Table 1 Design parameters of test data walls

Wall	CLBW01	CLBW02	CLBW03
Length (mm)	2690	3140	1640
Height (mm)	2208	1720	2208
Aspect ratio	0.82	0.55	1.35
Surface area (cm^2)	59395	54008	36211
Brick thickness (mm)		140	
Joint thickness (mm)	112		71
Mortar compressive strength (MPa)		17.4	
Units' compressive strength f_m (MPa)	10.2		7.6
Axial precompression (σ/f_m) (%)		5%	
Horizontal reinforcement ratio (%)		0.081	
Vertical reinforcement ratio (%)	0.4	0.32	0.5

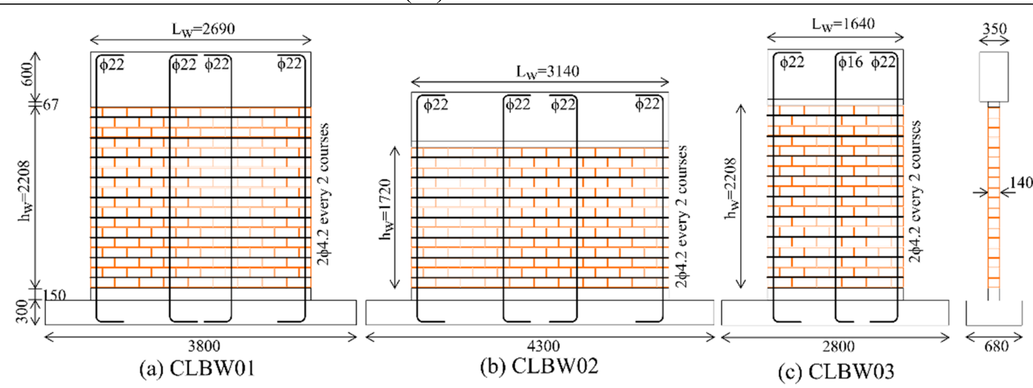

Figure 3. Walls geometry and design parameters for (a) CLBW01, (b) CLBW02, and (c) CLBW03.

DAMAGE PROGRESSION ANALYSIS

Table 2 presents the results of the different evaluated visible surface damage indexes at different loading states for the three case studies. Also, each index was evaluated at the loaded and unloaded state for the same maximum story drift ratio. Fig. 4 and Fig. 5 present the damage indexes' evolution as a function of story drift ratio at the loaded and unloaded states, respectively. It is worth mentioning that the figures plot from the first image at which damage was visually detected and that the instant at which the maximum load is achieved is indicated with a star marker. The damage begins to be visible at approximately 80% of shear resistance in the squared (CLBW1) and slender (CLBW3) walls, while the squat wall (CLBW2) starts showing damage at 64% of its lateral capacity. It is also noted that the CLBW1 wall is the first to reach its resistance and the only wall to exhibit damage at a drift of 0.2%. It is noted that damage evolution in CLBW02 and CLBW03 walls is slower than in wall CLBW01. Nonetheless, the increment rate is higher at the larger drift, which is most evident in the curves of the damage parameters in the unloaded state (Fig. 5). However, the increase in the visible damage for CLBW02 is much more abrupt than in the other walls when approaching to its peak shear resistance, which can be attributed to the influence of the aspect ratio because the lower the aspect ratio, the more fragile the response. In general, the squat wall shows more damage at its resistance than the other walls.

Table 2 Surface damage indexes for assessed walls.

Wall	Horizontal load (kN)	Story drift ratio (%)	Maximum crack width (mm)		Crack length (cm)		Bounding box area (cm^2)		Internal crack area (cm^2)	
			LS	US	LS	US	LS	US	LS	US
CLBW01	207.4	0.11	3.2	2.1	35.8	8.1	20.3	0.8	8	2
	221.8	0.13	4.2	3.2	189.4	36.6	5295.1	194.5	45	11
	255.0	0.20	4.2	4.2	425.7	139.2	6810.3	636.3	103	33
	257.2	0.26	5.3	4.2	738.7	335.9	11886.1	1376.0	187	90
	264.6	0.33	5.3	5.3	862.4	600.2	12830.8	3703.7	223	176
	238.9	0.37	9.5	6.4	1008.6	805.7	16691.5	6117.1	271	244
	206.7	0.44	10.6	8.5	1229.4	962.1	15766.8	9547.6	384	350
	123.3	0.52	11.7	8.5	1421.6	1200.1	20414.9	12935.5	514	482
CLBW02	269.9	0.24	4.9	2.6	296.2	14.1	3196.4	24.0	67	3
	293.0	0.30	6.2	4.9	461.3	49.8	6729.7	111.4	113	10
	326.7	0.36	6.2	4.9	587.9	114.5	6602.4	645.3	148	27
	367.8	0.42	6.2	4.9	760.2	171.9	8152.8	2382.5	185	42
	382.6	0.47	6.2	4.9	700.3	273.7	10479.9	2842.1	219	64
	407.1	0.52	6.2	6.2	896.1	764.2	13571.1	6916.7	305	178
	419.7	0.60	8.7	7.4	1345.6	791.1	19301.7	13327.5	472	304
CLBW03	126.0	0.23	2.8	2.8	112.0	52.9	549.3	51.6	18.2	8.4
	138.4	0.29	3.7	2.8	211.6	100.0	2248.0	89.0	35.7	16.1
	152.6	0.36	3.7	3.9	375.4	236.1	3083.9	402.6	63.7	38.3
	153.9	0.49	3.7	3.7	565.0	393.2	6305.8	889.8	96.3	65.7
	162.3	0.56	3.7	3.7	833.2	780.6	9313.0	5596.2	146.6	134.5
	150.1	6.2	3.9	4.6	1018.7	965.5	11195.9	7309.7	189.9	178.8
	112.4	5.5	7.4	6.5	910.1	1025.0	12068.6	8361.0	235.6	230.7

LS: Loaded State
US: Unloaded State

All index parameters of all three walls indicate a partial or even a complete "recovery" (or disappearance) of visible damage during the early stages of the test (see Fig. 4 and Fig. 5). This damage recovery capacity diminishes as the test progresses and the walls reach their peak shear resistance, resulting in an increment of the visible surface damage in the unloaded state. In particular, for the internal crack area (Fig. 4(b) and Fig. 5(b)), it is observed that the squat, squared, and slender wall can conceal up to 35%, 20%, and 10% of its surface damage once it reaches its peak shear resistance, indicating that aspect ratio can be linked to the crack closure phenomenon.

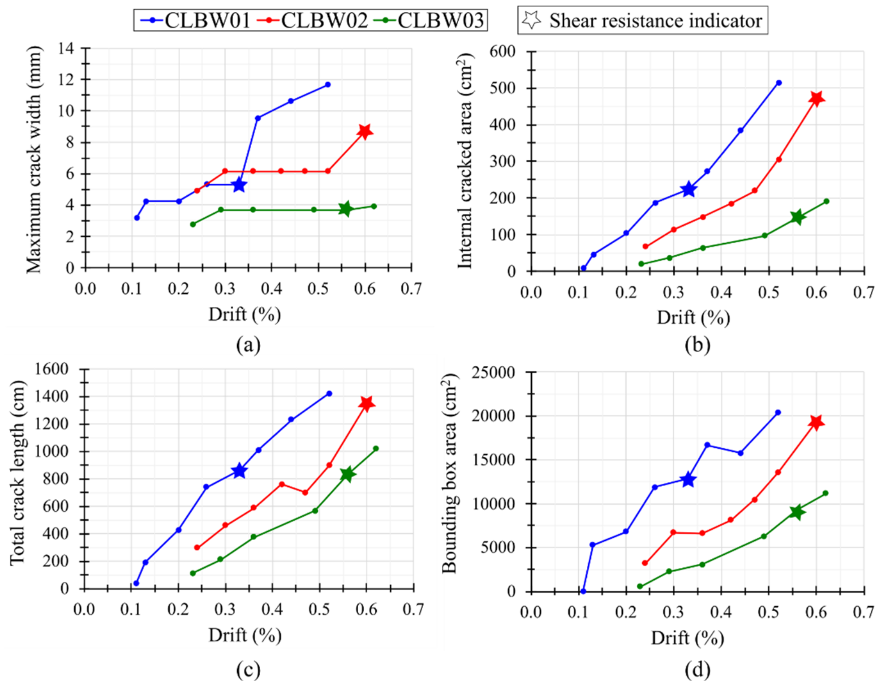

Figure 4. Loaded state damage progression comparison for all three walls for damage parameters: (a) Maximum crack width, (b) internal crack area, (c) total crack length, and (d) bounding box area.

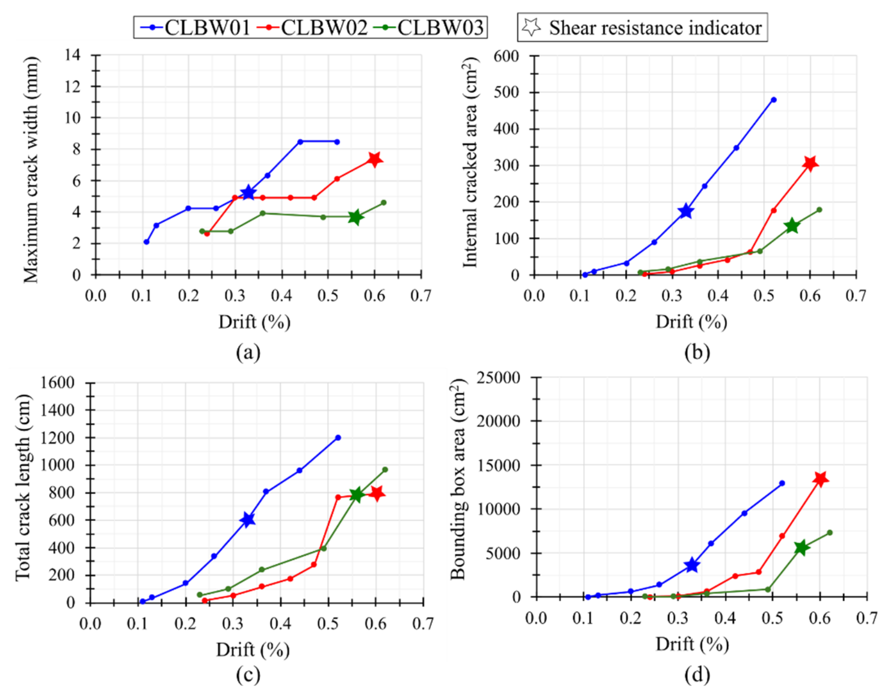

Figure 5. Unloaded state damage progression comparison for all three walls for damage parameters: (a) Maximum crack width, (b) internal crack area, (c) total crack length, and (d) bounding box area.

Maximum crack width

The evolution of the maximum crack width is shown in Fig. 6, where the story drift ratio at shear strength is also depicted for each wall. When analyzing the maximum crack width progression in the square wall CLBW01 (Fig.6(a)), a consistent increase is observed with each drift cycle. This trend suggests that maximum crack width could potentially serve as an indicator for estimating the level of damage in the wall. However, for the squat wall CLBW02 (Fig. 6(b)) and the slender wall CLBW03 (Fig. 6(c)), no clear progression in maximum crack width is observed.

Among the three walls, the CLBW2 wall demonstrates the most severe damage at its peak shear resistance, with maximum crack widths exceeding 8 mm (Fig. 6(b)). It also can be observed that there is a notable crack closure once the load is removed, which is more relevant in the square and squat walls. This behavior highlights a significant challenge in post-seismic damage evaluation because the visible crack width on an unloaded wall may be up to 40% narrower than the actual crack width, leading to potential underestimation of the true damage extent.

The lack of monotonic progression limits the usefulness of this index for estimating the extent of damage and for determining whether a wall has reached its peak shear resistance. Therefore, relying solely on maximum crack width for damage evaluation risks underestimating the actual damage.

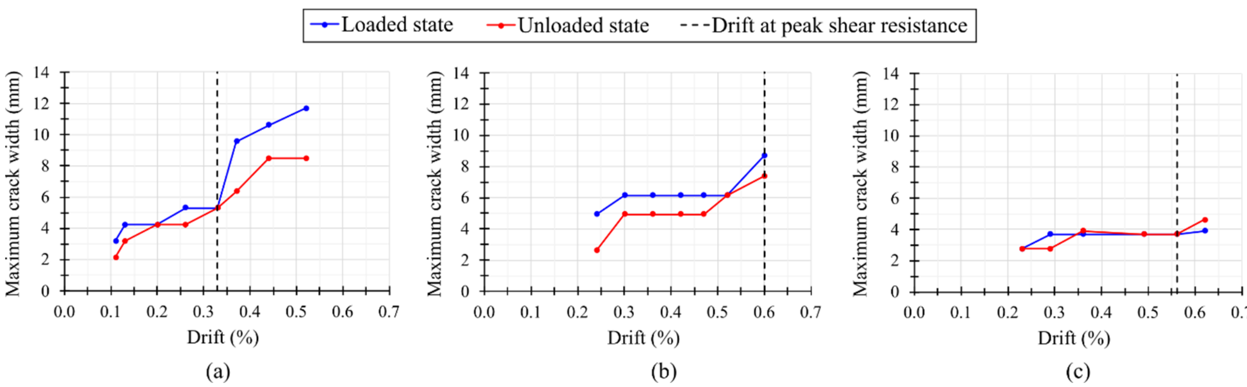

Figure 6. Maximum crack width versus drift for loaded and unloaded state for (a) square wall: CLBW01, (b) squat wall: CLBW02, and (C) slender wall: CLBW03.

Total crack length

The total crack length effectively identifies the damage progression in the three walls. It exhibits a steep slope, indicating significant differences in damage at each drift level. However, this index damage in the squat wall CLBW02 decreases at a drift of 0.47%, which is before the specimen reaches its shear resistance. This inconsistency can generate issues when assessing real walls.

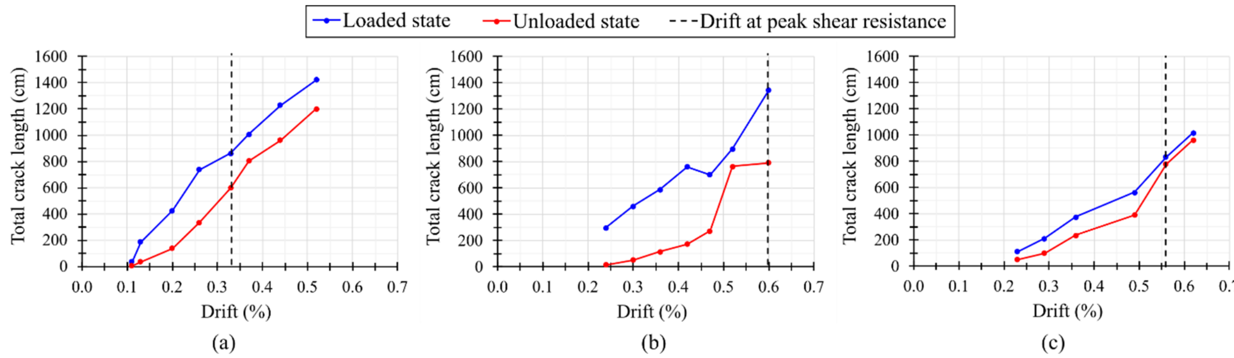

Figure 7. Total crack length versus drift for loaded and unloaded state for (a) square wall: CLBW01, (b) squat wall: CLBW02, and (C) slender wall: CLBW03.

Bounding box crack area

The bounding box area appears to be a suitable indicator of damage progression, exhibiting a distinct step and pronounced slope during both loaded and unloaded stages. However, decrements in this index are noticeable in the post-peak phase of the square wall. This can be attributed to the greater influence of individual cracks—or the interpretation of their extent—on the evaluation of crack patterns, especially at high damage levels and in non-linear behavior (after reaching its peak shear resistance). Consequently, this surface damage index seems to be suitable for pre-peak assessment.

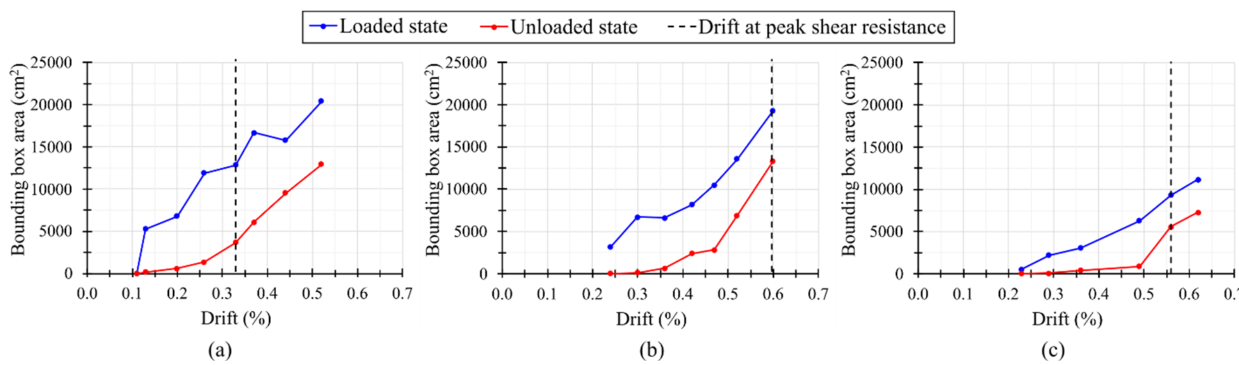

Figure 8. Bounding box area versus drift for loaded and unloaded state for (a) square wall: CLBW01, (b) squat wall: CLBW02, and (C) slender wall: CLBW03.

Internal crack area

The internal crack area in the square, squat, and slender walls (Fig. 9 (a), (b), and (c), respectively) appears to be a reliable parameter for estimating damage in both loaded and unloaded states. This parameter exhibits a steep slope, allowing for differentiation of the maximum experienced drift. Interestingly, this parameter reflects the crack closure phenomenon. The crack width reduction appears to decrease once the wall reaches its peak shear resistance, resulting in a diminished ability to recover visible surface damage. Despite this, the difference between the curves at loaded and unloaded states is smaller when compared to the other damage indexes. This situation suggests that this parameter is less affected by the crack closure phenomenon when the load is removed, as the index is less sensitive to small variations in individual crack widths.

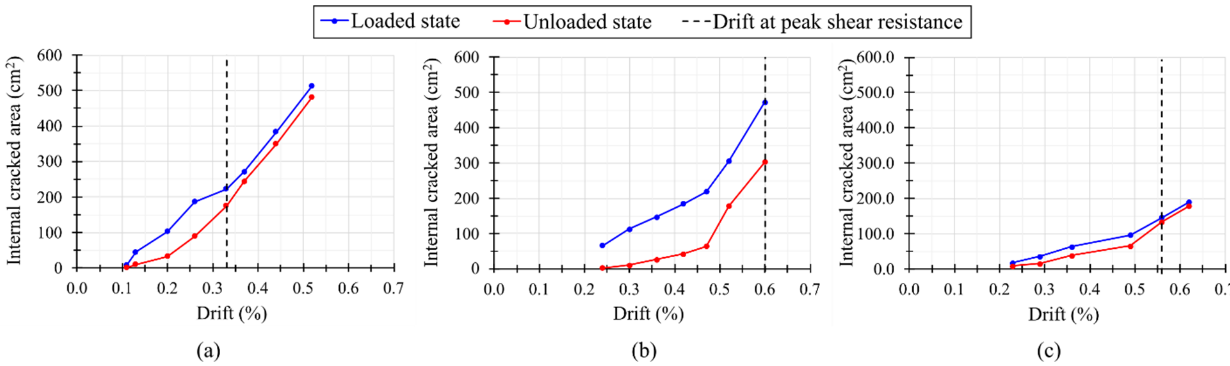

Figure 9. Internal crack area versus drift for loaded and unloaded state for (a) square wall: CLBW01, (b) squat wall: CLBW02, and (C) slender wall: CLBW03.

Overall, the internal crack area parameter proves to be the most promising for damage evaluation index among the assessed ones, demonstrating the steepest and most consistent damage progression across drift progression stages. It enables the estimation to distinguish if a wall reaches its shear strength and between the drift experienced before this point.

CONCLUSIONS

This study advanced the understanding of masonry shear wall behavior under cyclic loading by establishing a methodology for effectively quantifying crack patterns at peak drift and the residual cracks remaining after load removal. This allowed for a more in-depth quantification of the actual damage sustained by three tested walls under lateral loading, correlating demand parameters (horizontal load and story drift) with surface damage indexes (maximum crack width, crack length, internal crack area, and bounding box area) both in loaded and unloaded states.

It was observed that significant damage can persist even when visually undetectable. This underscores a critical issue in post-seismic evaluations: visible damage does not fully represent the actual damage incurred by a wall, leading to a potential underestimation of the real extent of damage. Moreover, the study highlights that maximum crack width is not a reliable indicator for estimating building damage during post-seismic evaluations. It was obtained that it failed to distinguish damage in the assessed squat and slender walls, a situation that limits its applicability as a damage evaluation index.

Additionally, it was observed that the three walls progressively lose their capacity to close visible cracks once the load is removed, particularly after reaching their shear resistance. This exposes more of the actual damage during post-seismic inspections on walls that exceeded their peak shear resistance. This phenomenon could be addressed by utilizing databases of images of severely damaged walls following seismic events, enabling the expansion and validation of this methodology.

The total crack length and internal crack area emerge as the most promising surface damage parameters for estimating damage, demonstrating a consistent progression and enabling clear differentiation between damage before and after reaching their peak shear resistance. Additionally, these parameters are less susceptible to human error in identifying crack patterns, as they account for a larger extent of the damage. Misinterpretations of individual cracks are negligible compared to the overall crack pattern damage captured by these parameters.

Future research will focus on validating these findings with a larger dataset and evaluating combinations of the most effective damage indexes identified in this study. Furthermore, the methodology is being extended to incorporate additional damage parameters and integrate AI algorithms for automated crack pattern detection. This will enable the development of robust correlations between visible damage and the overall damage level sustained by different wall typologies.

ACKNOWLEDGMENTS

The authors acknowledge the support of the EASER (Evolution Assessment of Seismic Risk) project under grant number ACT240044 from the National Agency for Research and Development (ANID). Sebastián Calderón also acknowledges the support of project FONDECYT No. 11230388 from the National Agency for Research and Development (ANID). The authors want to thank the financial support of the FONDEF Research Project No. ID17I10264. Gonzalo Lema wants to acknowledge the financial support from ANID-Subdirección de Capital Humano/Doctorado Nacional/2025-21251893.

REFERENCES

[1] Sandoval C, Calderón S, Almazan JL. (2018). Experimental cyclic response assessment of partially grouted reinforced clay brick masonry walls. *Bulletin of Earthquake Engineering*, 16:3127–52. https://doi.org/10.1007/s10518-018-0308-x.

[2] Murcia-Delso J, Shing PB. (2012). Fragility analysis of reinforced masonry shear walls. *Earthquake Spectra,* 28, 1523–47. https://doi.org/10.1193/1.4000075.

[3] The Japan Building and Disaster Prevention Association (JBDPA). (2015). *Guideline for Post-earthquake Damage Evaluation and Rehabilitation*.

[4] European Seismological Commission (ESC). (1998). *EMS-98. European macroseismic scale*. Luxembourg.

[5] Wang J, Ueda T. (2023). A review study on unmanned aerial vehicle and mobile robot technologies on damage inspection of reinforced concrete structures. *Structural Concrete,* 24, 536–62. https://doi.org/10.1002/suco.202200846.

[6] Cruz O, Pérez-Gavilán E. JJ, Flores C. L. (2019). Experimental study of in-plane shear strength of confined concrete masonry walls with joint reinforcement. *Eng Struct*, 182, 213–26. https://doi.org/10.1016/j.engstruct.2018.12.040.

[7] Loverdos D, Sarhosis V. (2022). Automatic image-based brick segmentation and crack detection of masonry walls using machine learning. *Autom Constr*, 140, 104389. https://doi.org/10.1016/j.autcon.2022.104389.

[8] [Calderón S, Sandoval C, Araya-Letelier G, Inzunza E, Arnau O. (2021). Influence of different design parameters on the seismic performance of partially grouted masonry shear walls. *Eng Struct*, 239, 112058. https://doi.org/10.1016/j.engstruct.2021.112058.

[9] Instituto Nacional de Normalización (INN). (2009). *NCh 1928. Of1993 Mod2009 : Albañilería armada - Requisitos para el diseño y cálculo*. Santiago.